A new ion cyclotron range of frequency scenario for bulk ion heating in deuterium-tritium plasmas: How to utilize intrinsic impurities in our favour

Ye.O. Kazakov[1], J. Ongena[1], D. Van Eester[1], R. Bilato[2], R. Dumont[3], E. Lerche[1], M. Mantsinen[4,5] and A. Messiaen[1]
[1] *Laboratory for Plasma Physics, LPP-ERM/KMS, EUROfusion Consortium member, Brussels, Belgium*
[2] *Max-Planck-Institut für Plasmaphysik, Garching, Germany*
[3] *CEA, IRFM, F-13108 Saint-Paul-lez-Durance, France*
[4] *Catalan Institution for Research and Advanced Studies, Barcelona, Spain*
[5] *Barcelona Supercomputing Center (BSC), Barcelona, Spain*

A fusion reactor requires plasma pre-heating before the rate of deuterium-tritium fusion reactions becomes significant. In ITER, radiofrequency (RF) heating of ^{3}He ions, additionally puffed into the plasma, is one of the main options considered for increasing bulk ion temperature during the ramp-up phase of the pulse. In this paper, we propose an alternative scenario for bulk ion heating with RF waves, which requires no extra ^{3}He puff and profits from the presence of intrinsic Beryllium impurities in the plasma. The discussed method to heat Be impurities in D-T plasmas is shown to provide an even larger fraction of fuel ion heating.

I. INTRODUCTION

In future fusion devices, radio frequency plasma heating with waves in the ion cyclotron range of frequencies (ICRF) is the only method capable of providing a significant fraction of bulk ion heating. This is due to the fact that electron cyclotron resonance heating, by definition, deposits wave energy to electrons. The same holds for the neutral beam injection systems because they will need to operate at rather high beam energies ($\sim$ 1 MeV) in order to reach the high-density plasma core.

As discussed in [1–3], preferential bulk ion heating during the ramp-up phase has a number of advantages. These include an improved control over the path to the burn phase and keeping away from the region where the interaction between thermal ions and thermal electrons is weak. As a result, reaching the operational point with higher Q can be done faster with less auxiliary heating power than for an electron heating scenario [1]. In addition, Tore Supra experiments demonstrated that higher levels of ion heating were accompanied by an improved energy confinement [2].

Applying ICRF power – somewhat counter-intuitively to its name – does not necessarily result in the dominant heating of bulk ions. In fact, depending on the chosen operational conditions (e.g., ICRF frequency, antenna phasing, plasma composition), the incoming RF power can be directly absorbed by various ion species, as well as by electrons. It is the latter condition one needs to fulfill in order to drive non-inductive current with ICRF system [4, 5]. However, channeling the RF power to be mostly absorbed by ions is not sufficient for bulk ion heating. In addition, one needs to avoid the formation of a high-energy ion tail due to ICRF. The critical energy $E_{\rm crit}$ of fast ions, at which the rate of loss of energy to the electrons and to the ions is equal, is given by $E_{\rm crit} = 14.8 A_{\rm fast} T_e \left(\sum_i X_i Z_i^2/A_i\right)^{2/3}$ [6]. Here, $A_{\rm fast}$ is the atomic mass of the energetic ions, T_e is the electron temperature, $X_i = n_i/n_e$, Z_i and A_i are the concentration, the charge state and the atomic mass of the thermal ion species, respectively. In order to achieve the resultant dominant heating of bulk ions, the energies of RF-accelerated minority ions should stay in the range of $E_{\rm crit}$ or below.

ICRF scenarios relevant for the D-T plasmas were discussed in detail in Refs. [1, 3, 4, 7], with the emphasis to ITER in, e.g., [8, 9]. Many of these scenarios were studied experimentally during the past D-T experiments in JET and TFTR tokamaks [10–14]. Currently, the second harmonic heating of tritium ions ($\omega = 2\omega_{c\rm T}$) is considered as the main ICRF scenario for the ITER burn-phase plasmas, and the fundamental heating of a small fraction of ^{3}He ions ($\omega = \omega_{c,^3\rm He}$), additionally puffed into the plasma, for the ramp-up low-temperature heating stage of the pulse. In JET, a fourfold increase of the neutron emission was observed when $X[^3\rm He] = 4\%$ was injected [11]. The higher reactivity observed with ^{3}He minority heating was due to the higher T_i reached. However, currently the supply of ^{3}He reduces and the industrial demand of this gas is progressively increasing [15].

In this paper, we introduce and discuss a promising alternative bulk ion heating scenario for the ramp-up phase in D-T plasmas. We will mainly focus on the applicability of the proposed scheme for ITER. Instead of using additionally puffed ^{3}He ions, we suggest to tune the RF system to heat predominantly intrinsic Beryllium (Be) impurities, which will be naturally present in ITER plasmas. Because of the larger atomic mass of Be, such ICRF heating is shown to provide an even larger fraction of bulk ion heating. Finally, we discuss how the current design of the ICRF system in ITER can be adapted to exploit the advantages of beryllium ICRF heating to their maximum. The proposed method is not restricted to the use of ^{9}Be only, but other impurities with a similar charge-to-mass ratio, such as ^{7}Li, ^{22}Ne, ^{40}Ar, etc. can be used as well. This is discussed in the last section of

the paper and is illustrated with a few examples.

II. THREE-ION (Be)-D-T ICRF SCENARIO

ICRF heating relies on launching the fast magnetosonic wave (FW) into the plasma by external antennas, typically located at the low field side (LFS) edge of the plasma. The FW propagation across the plasma is fairly well described by the well-known dispersion relation [16]

$$n^2_{\perp,\mathrm{FW}} \simeq \frac{(\epsilon_\mathrm{L} - n^2_\parallel)(\epsilon_\mathrm{R} - n^2_\parallel)}{\epsilon_\mathrm{S} - n^2_\parallel}, \tag{1}$$

where $n_{\perp,\parallel} = ck_{\perp,\parallel}/\omega$ is the perpendicular/parallel FW refractive index, and the tensor components ϵ_S, ϵ_L and ϵ_R are those given by Stix [17].

The FW power is absorbed by ions, when the wave crosses the ion cyclotron (IC) resonance ($\omega = \omega_{ci}$) and IC harmonic ($\omega = N\omega_{ci}, N \geq 2$) layers. Electron absorption is also possible via a combination of electron Landau damping and transit time magnetic pumping, especially at high electron beta. Electron heating can also occur via mode conversion of the incoming FW to shorter wavelength modes, which takes place at the ion-ion hybrid resonance(s) in multi-ion plasmas [18].

In general, the FW is elliptically polarized and its electric field can be decomposed as a sum of two components: the left-hand polarized component E_+, which rotates in the sense of ions in the magnetic field, and the right-hand polarized component E_- that is aligned with electron rotation. In his seminal paper [19], Stix showed that the absorbed RF power by thermal ions is almost merely due to the left-hand E_+ component. One should note here that it is the plasma, rather than the ICRF system, which defines the wave polarization and imposes the ratio between E_+ and E_- [19]

$$\left|\frac{E_+}{E_-}\right| \simeq \left|\frac{\epsilon_\mathrm{R} - n^2_\parallel}{\epsilon_\mathrm{L} - n^2_\parallel}\right|. \tag{2}$$

Though the characteristic $n_\parallel$, which appears in Eqs. (1) and (2), can be varied by changing the ICRF antenna phasing and operational frequency, the main contribution to Eq. (2) generally comes from the tensor elements.

One option for ion absorption in fusion plasmas is applying IC harmonic heating ($N \geq 2$), $|E_+/E_-| \simeq (N-1)/(N+1)$. This damping mechanism is, however, a finite Larmor radius effect and hence not appropriate for the beginning of the heating phase in a reactor (low densities and low temperatures). Another option – known as minority heating in two-ion plasmas [19] – is to heat a small fraction of resonant minority ions at their fundamental IC resonance. This scenario typically shows the best performance at minority concentrations of $X_\mathrm{mino} = n_\mathrm{mino}/n_e \approx 3-10\%$ and has been routinely used for plasma heating. Though minority heating has a quite strong single-pass absorption (SPA), especially for hydrogen minority heating in deuterium majority plasmas, the ratio of the left- to the right-hand polarization at the IC resonance of minority ions is limited [11]

$$\left|\frac{E_+}{E_-}\right|_{\omega=\omega_{c2}} \approx \left|\frac{\mathcal{Z}_2 - \mathcal{Z}_1}{\mathcal{Z}_2 + \mathcal{Z}_1}\right| < 1, \tag{3}$$

and the FW is mostly right-hand polarized. Here, we introduced the notation $\mathcal{Z}_i = (Z/A)_i$, which stands for the ratio of the charge state to the atomic mass for the ion species. By way of example, for (H)-D heating $|E_+/E_-| \approx 1/3$, which is enough to obtain an efficient single-pass absorption at $X_\mathrm{H} \approx 5\%$ (typical H concentration used in the experiments). Yet, two-ion ICRF minority heating at much lower minority concentrations (e.g., $X_\mathrm{mino} \ll 1\%$) is usually characterized by very poor wave absorption and for this reason is not often used in practice.

In our recent paper [20], we presented a method to maximize the E_+ component and, subsequently, to achieve a strong ion absorption at very low minority concentrations ($\sim 1\%$ or lower). This enhanced ion absorption requires the presence of three ion species in a plasma (with a different Z/A): two main ion species (X and Y) and a third resonant ion species (Z), present at a very small concentration. The key idea is to locate the left-hand polarized fast wave L-cutoff, which is defined by the condition $\epsilon_\mathrm{L} = n^2_\parallel$ and which largely enhances the associated RF field component E_+, close to the fundamental cyclotron resonance of the minority ion species Z. This matching can be achieved by adjusting the density ratio between the two main ion species Y:X.

Note that not all ICRF scenarios with three ion species can lead to E_+ enhancement. One of the necessary conditions is that

$$\min\{\mathcal{Z}_1, \mathcal{Z}_2\} < \mathcal{Z}_3 < \max\{\mathcal{Z}_1, \mathcal{Z}_2\}, \tag{4}$$

i.e. the resonant minority ions, one aims to heat, should have a cyclotron resonance located between the IC resonances of the two bulk ion species. The main ICRF scenario for bulk ion heating in D-T ITER plasmas, viz. (^{3}He)-DT, does not belong to this list since $\mathcal{Z}_3 > \mathcal{Z}_{1,2}$.

Tungsten and beryllium have been chosen as the plasma-facing components for ITER. Accordingly, the carbon wall was replaced with the ITER-like wall in JET since 2011. Therefore, JET and ITER plasmas will unavoidably include a non-negligible amount of Be impurities. For example, $X_\mathrm{Be} = 1-2\%$ is estimated as the background Be level in JET plasmas [21, 22]: the measured core $Z_\mathrm{eff} \approx 1.2$ yields $X_\mathrm{Be} \simeq 1.4\%$ for the residual carbon content of about $X_\mathrm{C} \simeq 0.1\%$ (note that $Z_\mathrm{eff} \approx 1.1$ yields $X_\mathrm{Be} \approx 0.6\%$). A charge-to-mass ratio of the fully-ionized beryllium ions ($A = 9$, $Z = 4$) satisfies the condition of Eq. (4), $\mathcal{Z}_\mathrm{T} < \mathcal{Z}_\mathrm{Be} < \mathcal{Z}_\mathrm{D}$, and therefore (Be)-D-T scenario belongs to the set of three-ion ICRF heating scenarios. Though in Ref. [23] it was correctly outlined that the application of D-T mode conversion heating could be hampered due to the Be presence, our recent results [20] show that the impact of the three-ion

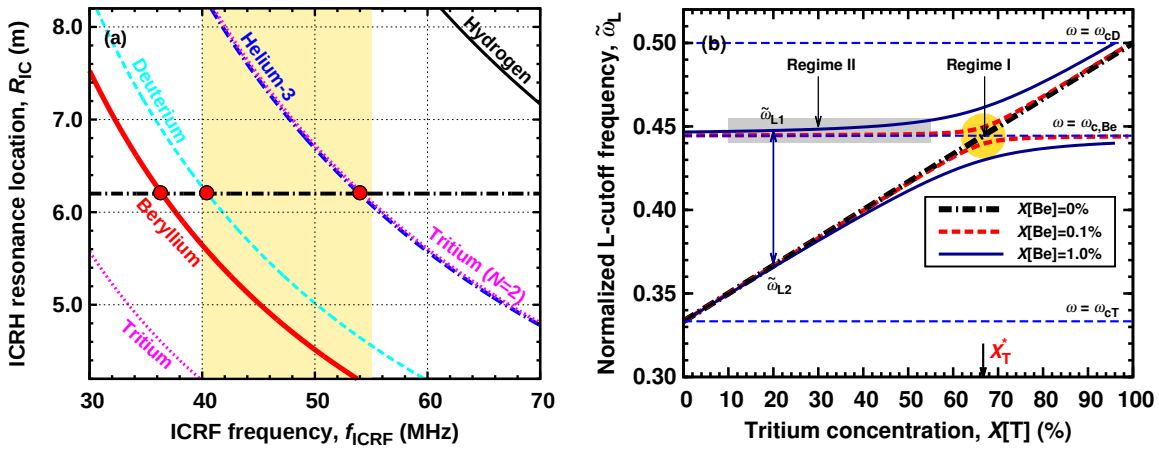

FIG. 1. (a) Location of the IC resonances in the ITER plasma at the full magnetic field ($B_0 = 5.3$ T). The official ITER frequency range for the ICRF system $f = 40 - 55$ MHz is highlighted. (b) The normalized L-cutoff frequency, $\tilde{\omega}_L = \omega_L/\omega_{cH}$ as a function of tritium and beryllium concentrations in a (Be)-D-T plasma.

ICRF scenarios can be reverted and such scenarios have a great potential for fusion research (fast-ion generation and bulk plasma heating). Below, we explore the features of the (Be)-D-T ICRF scenario in ITER-like plasmas and compare the potential of bulk ion heating for this scenario with the more traditional (^{3}He)-DT scheme.

III. (Be)-D-T HEATING IN ITER

Figure 1(a) shows the location of the main IC resonances in ITER ($R_0 = 6.2$ m, $a = 2.0$ m) as a function of the ICRF frequency for the nominal magnetic field $B_0 = 5.3$ T. In ITER, two ICRF antennas mounted in mid-plane ports are envisaged to operate within the range $f = 40 - 55$ MHz [24, 25]. Such a frequency range for ITER provides central $N = 1$ and $N = 2$ heating for ^{3}He and T ions at $f \approx 53$ MHz, and fundamental IC heating of D ions at $f \approx 40$ MHz (for (D)-T pulses). We also depict the location of the IC resonance of Be impurities (red solid line) in Fig. 1. One can see that the distance between the Be and D cyclotron resonances is about 70 cm, and a frequency only slightly below the official minimum ICRF frequency for ITER $f \approx 36-37$ MHz is required to locate the Be resonance close to the plasma center. A frequency $f = 37$ MHz is used throughout the paper, unless otherwise stated. According to the arguments presented in the last section of this paper, the ICRF system in ITER can operate at this frequency, without any dramatic changes to the present design. As will also be discussed below, operation at $f = 40$ MHz can still provide dominant Be heating at the price of yielding reasonably off-axis power deposition.

Depending on the impurity concentration, one can distinguish two different regimes of the three-ion ICRF heating. If the concentration of Be ions is extremely small ($X_{Be} \ll 1\%$), the optimal T concentration for maximizing Be absorption can be found from Eq. (7) of Ref. [20], viz. $X^*_T \approx (\mathcal{Z}_{Be} - \mathcal{Z}_T)/(\mathcal{Z}_D - \mathcal{Z}_T) \approx 67\%$ (D:T $\simeq$ 1:2). At such X_T, the L-cutoff in D:T plasmas (see dashed-dotted line in Fig. 1(b)) and the cyclotron resonance of Be impurities intersect. However, in three-ion Be-D-T plasmas with a finite X_{Be}, the L-cutoff can not cross the IC resonance of Be. This is clear from the equation for the normalized L-cutoff frequency ($\tilde{\omega}_L = \omega_L/\omega_{cH}$), which can be written as follows [26]

$$\frac{X_T}{\tilde{\omega}_L - \mathcal{Z}_T} + \frac{X_D}{\tilde{\omega}_L - \mathcal{Z}_D} + \frac{4X_{Be}}{\tilde{\omega}_L - \mathcal{Z}_{Be}} \simeq 0. \qquad (5)$$

Note that any solution of Eq. (5) can be translated into the corresponding radial coordinate of the L-cutoff via $R_L \approx R_0\,\tilde{\omega}_L\,15.25\,B_0(\mathrm{T})/f(\mathrm{MHz})$. In fact, as follows from Fig. 1(b), in the vicinity of $\omega = \omega_{c,Be}$, the curve for $\tilde{\omega}_L$ splits in two, and generally there are two meaningful solutions of Eq. (5) at a given X_T and X_{Be}. Far from the region of the resonant crossing ($X_T \approx X^*_T$), they can be approximated with expressions

$$\begin{aligned} \tilde{\omega}_{L1} &\approx \mathcal{Z}_{Be} + \frac{4(\mathcal{Z}_D - \mathcal{Z}_{Be})X^*_T X_{Be}}{X^*_T - X_T}, \\ \tilde{\omega}_{L2} &\approx \mathcal{Z}_T + (\mathcal{Z}_D - \mathcal{Z}_T)X_T - \frac{4(\mathcal{Z}_D - \mathcal{Z}_{Be})X_T X_{Be}}{X^*_T - X_T}. \end{aligned} \qquad (6)$$

In the vicinity of $X_T \approx X^*_T$, these approximations are not valid. For very low $X_{Be} \ll 1\%$, the gap between two solutions $\tilde{\omega}_{L1}$ and $\tilde{\omega}_{L2}$ is small, and the optimal conditions for the ICRF heating occur at the tritium concentration X^*_T, at which the two asymptotics intersect. We have depicted such conditions as 'Regime I' in Fig. 1(b), and this heating regime has been suggested for fast-ion generation with ICRF and studied in detail in [20].

However, for higher Be concentrations ($X_{Be} \sim 1\%$), at $X_T \simeq X^*_T$ the gap between ω_{L1} and $\omega_{c,Be}$ is already quite large. As a result, the distance between the region with the enhanced E_+ and Be cyclotron resonance

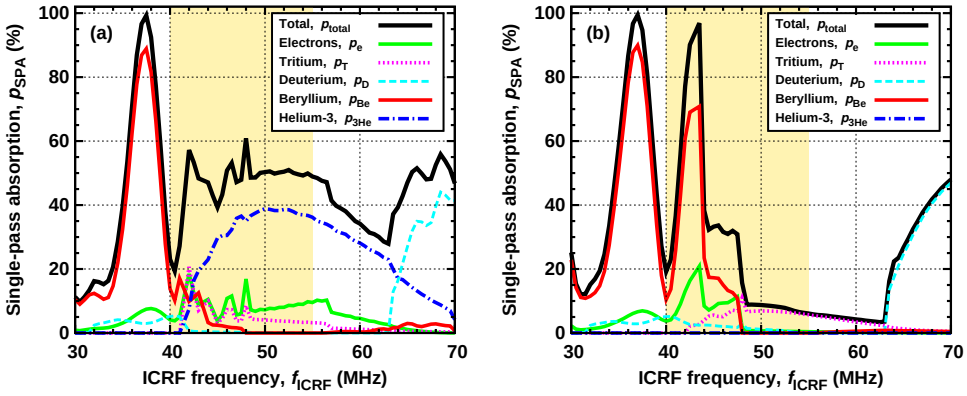

FIG. 2. Single-pass absorption coefficients as a function of the ICRF frequency for the ITER ramp-up phase as computed by TOMCAT ($B_0 = 5.3$ T, D:T=1:1, $T_0 = 4$ keV, $n_{e0} = 6 \times 10^{19}$ m^{-3}, $k_{\|}^{(ant)} = 3$ m^{-1}): (a) (^{3}He)-DT scenario ($X_{^3\mathrm{He}} = 2\%$, $X_{\mathrm{Be}} = 1\%$); (b) (Be)-D-T scenario (no $X_{^3\mathrm{He}}$, $X_{\mathrm{Be}} = 1\%$).

exceeds the Doppler width of the IC resonance, and minority ion absorption at such conditions significantly decreases. Thus, as already noted in [20], the optimal tritium concentration for maximizing Be absorption shifts towards lower values of X_{T}. These conditions, which are schematically depicted as 'Regime II' in Fig. 1(b), correspond to the conditions of (Be)-D-T heating in ITER and will be studied in this paper.

We start with a comparison between the (^{3}He)-DT and (Be)-D-T ICRF scenarios by evaluating the single-pass absorption coefficients (a fraction of the incoming RF power absorbed by plasma species as the wave propagates from the LFS edge to the high field side edge) as a function of ICRF frequency. These are computed with the TOMCAT code [27] and are depicted in Fig. 2. For both scenarios, the background $X_{\mathrm{Be}} = 1\%$ and an optimal D:T=1:1 ratio is assumed. For the ^{3}He minority scenario, shown in Fig. 2(a), an additional $X_{^3\mathrm{He}} = 2\%$ is considered. Because of the plasma dilution, the concentration of fuel D-T ions for this scenario is somewhat lower than for Be minority heating ($X_{\mathrm{D,T}} = 46\%$ vs. $X_{\mathrm{D,T}} = 48\%$). We focus on the ITER ramp-up phase, when the plasma density and temperatures are rather low and the rate of D-T fusion reactions is small, such that the contribution of alpha-particles to the power balance is negligible. As baseline conditions, we consider $T_0 = 4$ keV, $n_{e0} = 6 \times 10^{19}$ m^{-3}, $n_{\mathrm{tor}} = 27$ ($k_{\|}^{(ant)} = 3$ m^{-1}). Such a value of the FW parallel wavenumber is representative for the $[0; 0; \pi; \pi]$ toroidal phasing of the ITER ICRF antenna [8, 28]. An influence of the antenna toroidal spectrum on ICRF heating scenarios in ITER was studied in [9, 28]. For the (^{3}He)-DT scenario, two modelling approaches (full-spectrum computations and retaining only the dominant toroidal mode number) were shown to give almost identical results (see Table II of Ref. [28]). Hence, for proof-of-principle computations which we present in this paper, we have adopted a simpler approach and considered only the dominant wavenumber.

As follows from Fig. 2, for the considered conditions the single-pass absorption for the ^{3}He minority scenario is $p_{^3\mathrm{He}} \approx 40\%$ at $f \approx 50$ MHz. The single-pass absorption for the Be heating scenario can be stronger $p_{\mathrm{Be}} \approx 90\%$, if operating at a lower frequency $f \approx 37$ MHz. Note that $p_{^3\mathrm{He}} \approx 40\%$, which is computed for the (^{3}He)-DT scenario, does not mean poor ICRF heating. Typically, such p_{SPA} is still high enough for having good multi-pass ICRF performance ($p_{\mathrm{SPA}} = 40-50\%$ reflects that the FW needs to pass the resonant layer several times before the power is absorbed). Note that operation at $f \approx 43$ MHz (secondary peak of Be absorption in Fig. 2(b)) is not very promising since then the RF power is deposited appreciably off-axis ($(r/a)_{\mathrm{Be}} \approx 0.5$, cf. Fig. 1(a)).

There is another criterion to consider: one needs to make sure that the ICRF scheme in question is robust with respect to changes in the D:T ratio and Be concentration. Since the results shown in Fig. 2 were computed with a 1D code, which neglects a number of effects intrinsic for the tokamak geometry such as a finite poloidal magnetic field, a more sophisticated modelling with the 2D full-wave codes TORIC [29, 30] and EVE [31] was done to increase the degree of realism. Note that contrary to the 1D computations, in 2D modelling (since the tokamak vessel acts as a Faraday cage) all the RF power is eventually absorbed in the plasma, and the computed absorption coefficients reflect the relative strength of various damping mechanisms. For the 2D computations we adopted a Shafranov shift of 10 cm and applied $B_0(R_0 = 6.2\ \mathrm{m}) = 5.4$ T such that the magnetic field at the magnetic axis is 5.3 T as for the 1D computations. There is generally a good agreement between TORIC and EVE results. Figure 3(a) shows that damping of the RF power on Be impurities is the dominant absorption channel ($p_{\mathrm{Be}} > 60\%$) for a wide range of tritium concentrations, namely $X_{\mathrm{T}} = 20 - 60\%$. This is in line with the arguments behind Fig. 1(b) and discussions above. The remaining incoming RF power is almost equally split between fuel D ions and electrons.

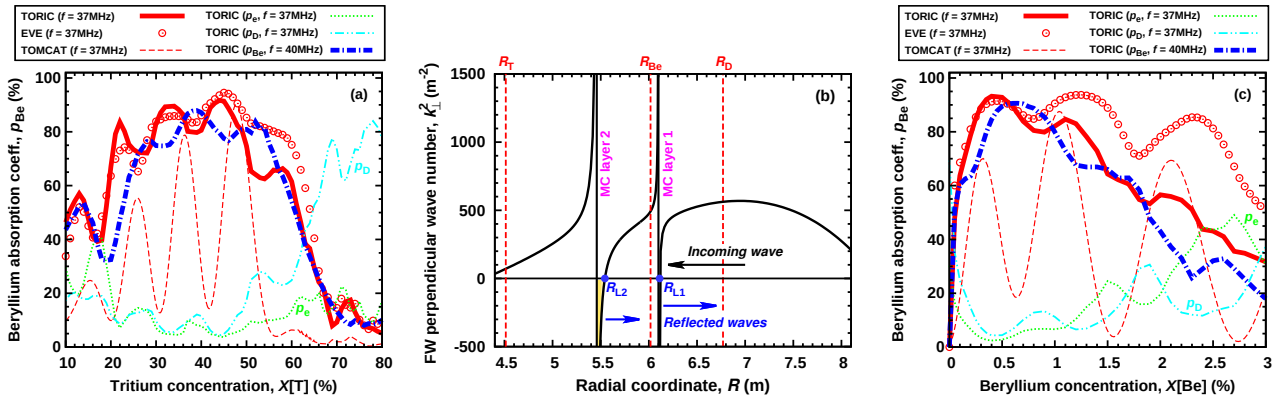

FIG. 3. Beryllium impurity ICRF heating scenario, (Be)-D-T: (a) Absorption coefficients as a function of tritium concentration ($X_{\rm Be} = 1\%$), as computed by TORIC, EVE and TOMCAT; (b) Radial dependence of the real part of $k^2_{\perp,\rm FW}$ ($X_{\rm Be} = 1\%$, $X_{\rm D} = X_{\rm T} = 48\%$); (c) $p_{\rm abs}$ vs. beryllium concentration (D:T=1:1).

One can also notice a modest oscillatory behavior of $p_{\rm Be}$ in Fig. 3(a). TORIC computations predict that the maxima of Be absorption are reached at $X_{\rm T} \approx 22\%, 34\%$, 44% and 58%, and minima at $X_{\rm T} \approx 28\%, 39\%$ and 54%, respectively. This occurs due to a constructive/destructive interference effect. Similar to the structure considered in [32–35], for (Be)-D-T plasmas there are two MC layers located in the plasma (see Fig. 3(b)). As noted, Eq. (5) has two meaningful solutions: the first L-cutoff $R_{\rm L1}$ is located close the IC resonance of Be ions, $R_{\rm Be}$ (to the lower magnetic field side of that) and the second $R_{\rm L2}$ to the higher field side of $R_{\rm Be}$. In contrast to 'Regime I' heating, when the impurity concentration is too small to form the two well-separated MC layers, for this regime the RF power is not very efficiently absorbed, when the FW passes through the first MC layer and Be cyclotron resonance ($p_1 \simeq 30\%$). The transmitted FW ($\mathcal{T} \simeq 40\%$) reaches the second MC layer and is almost entirely reflected back at $R_{\rm L2}$. As a result, the interference of the two reflected waves determines the resultant reflection and absorption coefficients. Analytical formulae describing the constructive/destructive interference effect for minority heating regime were derived in [36]. According to Eqs. (5) and (6) of [36], the minority ion absorption varies between $p_{i,\rm min} \approx 13\%$ and $p_{i,\rm max} \approx 99\%$, depending on the phase difference $\Delta\phi$ between the two reflected waves. An average single-pass absorption coefficient is then $\bar{p}_i = p_1 + \mathcal{T}(1-\mathcal{T}) \approx 54\%$.

The two MC layers shown in Fig. 3(b) have essentially different radial width. Whereas for the first layer $\Delta_{\rm MC1} \simeq 1 - 1.5$ cm, the second MC layer is much wider $\Delta_{\rm MC2} \simeq 10$ cm and is, thus, non-transparent for the wave propagation. As the concentration of T ions is gradually decreased from $X^*_{\rm T}$, the distance between $R_{\rm L2}$ and the first MC layer increases (see Eq. (6))

$$\Delta R_{12} \simeq [(\mathcal{Z}_{\rm Be} - \mathcal{Z}_{\rm T}) - (\mathcal{Z}_{\rm D} - \mathcal{Z}_{\rm T})X_{\rm T}]\, R_{\rm Be}/\mathcal{Z}_{\rm Be} \approx \approx (1 - 3X_{\rm T}/2)\, R_0/4.$$

Every new maximum/minimum shown in Fig. 3(a) marks a case, when the phase term $\Phi \simeq \bar{k}_{\perp,\rm FW}\Delta R_{12}$ has changed by $\delta\Phi = \pi/2$, i.e. the radial distance R_{12} has increased roughly by a quarter of the average FW perpendicular wavelength. Naturally, such oscillations are much more pronounced in 1D (TOMCAT) computations, and the modulation amplitude for 2D $p_{\rm abs}$–computations is much smaller. Since $\bar{k}_{\perp,\rm FW} \simeq (\omega_{\rm pH}/c)\mathcal{Z}_{\rm Be}\left(\sum_i X_i A_i\right)^{1/2} \approx 0.7(\omega_{\rm pH}/c)$ with $\omega_{\rm pH} = (4\pi n_e e^2/m_{\rm H})^{1/2}$, a characteristic tritium variation, marking the transition from the maximum of $p_{\rm Be}$ to the minimum and vice versa, has been derived

$$\delta X_{\rm T} \simeq \frac{8\pi}{3\bar{k}_\perp R_0} \approx 0.27/(\sqrt{n_{e,20}}\, R_0\,({\rm m}))\,. \qquad (7)$$

Here, $n_{e,20}$ is the plasma density expressed in the units 10^{20} m^{-3} and R_0 is the major radius of the machine in meters.

Accurate measurements of the concentration of Be impurities in the plasma center are not readily available. Though we fixed $X_{\rm Be} = 1\%$ in our previous computations, one should consider this value only as a rough estimate. Figure 3(c) depicts the sensitivity of the 2D absorption coefficients as a function of $X_{\rm Be}$. The concentrations of fuel D and T ions for every numerical run were adjusted accordingly to obtain an optimal D:T=1:1 mixture. Our results show that the RF power is absorbed mostly by Be impurities within a fairly wide range $X_{\rm Be} \approx 0.1\% - 2\%$. For the considered conditions, the Be absorption has peaks around $X_{\rm Be} \approx 0.5\%$ and 1.2%, and tends to decrease at higher concentrations. At $X_{\rm Be} \gtrsim 2.4\%$, electron absorption starts to be equally important. Should ITER plasmas include high Be levels $X_{\rm Be} \gtrsim 2.5 - 3\%$, this will result in a reduced Be absorption. However, under these conditions at least 20% of the output fusion power will be lost due to the fuel dilution. A general conclusion, which one can draw from studying Figs. 3(a) and (c), is that for the given ICRF frequency $f = 37$ MHz Be absorption is the dominant

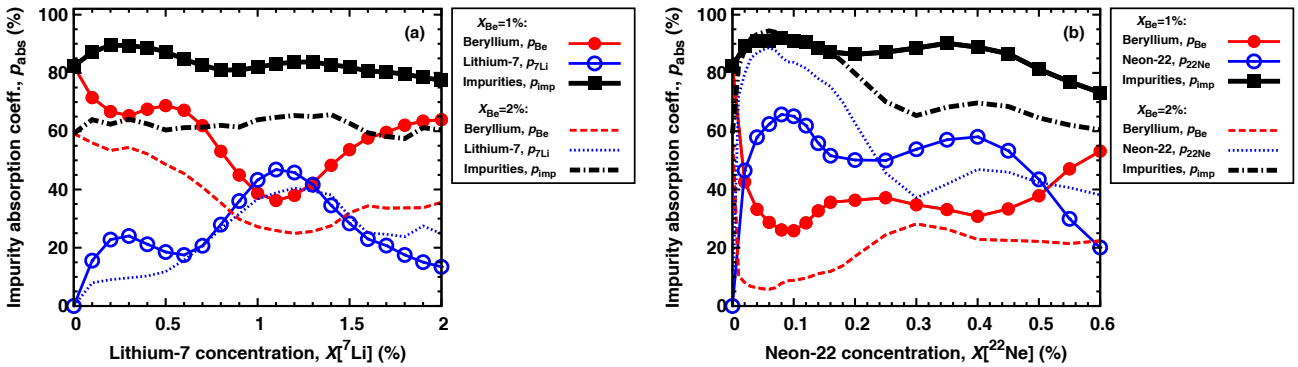

FIG. 4. An effect of extra impurity species with $Z/A \approx 0.43-0.45$: absorption coefficients as a function of (a) ^{7}Li and (b) ^{22}Ne concentrations. Lines with symbols correspond to the case $X_{\rm Be} = 1\%$ (data for $X_{\rm Be} = 2\%$ case is shown with lines only).

TABLE I. Location of IC resonant layers $\omega = \omega_{ci}$ for bulk ion and impurity species, $x_{\rm IC} = R_{\rm IC} - R_0$ ($R_0 = 6.2$ m, $a = 2.0$ m).

	Ion species	T	^{7}Li	Be	^{22}Ne	D, ^{20}Ne
37 MHz	$x_{\rm IC}$ (m)	-1.69	-0.40	-0.19	-0.05	0.57
	$x_{\rm IC}/a$	-0.85	-0.20	-0.09	-0.03	0.28
40 MHz	$x_{\rm IC}$ (m)	-2.03	-0.84	-0.64	-0.51	0.06
	$x_{\rm IC}/a$	-1.01	-0.42	-0.32	-0.26	0.03

TABLE II. RF power split (direct heating and collisional redistribution) for the (^{3}He)-DT and (Be)-D-T ICRF scenarios.

	Electrons	^{3}He/Be ions	Bulk ions
a) (^{3}He)-DT scenario:			
Direct RF heating	9%	76%	14%
Collisional redistribution (10 MW)	29%	5%	62%
Collisional redistribution (20 MW)	43%	4%	50%
b) (Be)-D-T scenario:			
Direct RF heating	6%	82%	12%
Collisional redistribution (10 MW)	10%	9%	81%
Collisional redistribution (20 MW)	17%	7%	76%

channel of the RF absorption for a wide range of realistic plasma conditions in ITER.

The dashed-dotted lines shown in Fig. 3(a) and (c) depict the absorption coefficient by Be impurities computed with TORIC for $f = 40$ MHz. It is clear that Be absorption dominates over the other damping mechanisms for this ICRF frequency as well.

The presence of high-Z impurities like tungsten has a small impact on the (Be)-D-T scenario. A typical charge state for W in the plasma core is $Z \simeq 40-50$ [37], and such impurities have $(Z/A)_{\rm W} \approx 0.2-0.3$, which is very different to $(Z/A)_{\rm Be}$. On the contrary, impurities with a charge-to-mass ratio close to that of Be ions, e.g. $^7Li^{3+}$, could have a non-negligible effect on RF power absorption. Figure 4(a) shows absorption coefficients by Be and ^{7}Li impurities computed by TORIC for D:T=1:1 plasmas. As follows from this figure, the total absorption of RF power by two different impurity species $p_{\rm imp} = p_{\rm Be} + p_{^7{\rm Li}}$ remains nearly constant. Since Z/A for Be and ^{7}Li ions is not identical, the IC resonant layers of these impurities are separated by a distance about 20 cm, and therefore the radial position of the maximum of impurity absorption is somewhat different (peaking at $r/a \simeq 0.1$ and 0.2, respectively).

Another impurity species relevant for the studied ICRF scenario is the second most abundant isotope of neon, $^{22}Ne^{10+}$ (natural abundance 9.3%). In fact, for $f = 37$ MHz the IC resonance of ^{22}Ne impurities is located closer to the plasma center than the Be resonance (see Table I). As a result, FW excited by a LFS antenna approaches the resonance of ^{22}Ne ions first and hence one can tune most of RF power to be absorbed by neon ions. This is clearly illustrated in Fig. 4(b), where a scan in $X_{^{22}{\rm Ne}}$ is made for two beryllium background levels. E.g., for $X_{\rm Be} = 1\%$, adding as little as 0.02% of ^{22}Ne ions allows changing the dominant impurity absorption channel and bringing the absorption region even closer to the plasma center. Another stable isotope of neon, ^{21}Ne, is very rare (abundance 0.27%), and for the considered conditions not absorbing much of RF power. A preliminary conclusion one can draw from Figs. 4(a) and (b) is that having extra impurity species with a similar $Z/A \approx 0.43-0.45$ and IC resonant layers located close to Be resonance ($\left|x_{\rm IC}^{\rm (imp)} - x_{\rm IC}^{\rm (Be)}\right|/a \simeq 0.1$, see Table I) is not hindering the here considered heating scenario.

Comparison of the collisional power redistribution

Finally, we compare the collisional power redistribution for the ^{3}He and Be minority heating scenarios. As outlined in the introduction, the critical energy, at which an equal amount of absorbed RF power collisionally goes to bulk ions and electrons, increases with the atomic mass of the energetic particles: $E_{\rm crit}[^3{\rm He}] \approx 25T_e$ and $E_{\rm crit}[{\rm Be}] \approx 74T_e$, respectively. Hence, at comparable ICRF power densities, a stronger bulk ion heating is expected for the (Be)-D-T scenario.

In terms of the fraction of RF power absorbed directly by various plasma species, the two ICRF scenarios are

very similar. As follows from Table II, minority ions (^{3}He and Be, respectively) absorb about $75-80\%$ of the launched power, $<10\%$ of the RF power is deposited on electrons, and the rest $10-15\%$ is absorbed by bulk D and T ions. Using the RF power densities evaluated by TORIC, the Fokker-Planck solver SSFPQL [38] was used to estimate the collisional power redistribution between the species. For $P_{\rm ICRF}=10$ MW of coupled RF power, the fraction of bulk ion D-T heating is 62% for the (^{3}He)-DT scenario. This reduces to 50% for 20 MW of coupled RF power. The electron heating fraction is computed to be 29% and 43%, respectively. Note also that a finite amount of RF power eventually goes to heat minority ^{3}He and Be impurities. The computed results are quite similar to those reported in Ref. [9] (however, a higher plasma density and temperatures were used in those simulations).

For the (Be)-D-T scenario, the fraction of bulk ion heating is larger. For 10 MW of coupled RF power, about 80% eventually ends up in bulk D-T ions and only 10% in electrons. Increasing the coupled RF power does not result in any significant reduction of p_i. For $P_{\rm ICRF}=20$ MW, fuel D and T ions still absorb 76% of the coupled power and the fraction of electron heating increases only up to 17%.

Note that if extra natural neon (with natural abundances of isotopes) is puffed into the plasma, this can result in a somewhat higher electron heating fraction. For example, adding 0.5% of natural neon gas ($\Delta Z_{\rm eff}\approx 0.5$) brings only $\sim 0.05\%$ of ^{22}Ne ions. As shown in Fig. 4(b), ^{22}Ne ions can absorb a lot of RF power even at such very low concentrations. Subsequently, a tail of high-energy ions is expected to develop in the ^{22}Ne distribution function which can collisionally transfer a significant fraction of power to the electrons. Such a more complicated multi-impurity option deserves a further detailed study (this scenario is also numerically more challenging because of the multiple ion-ion hybrid layers present in the plasma) and the corresponding results will be reported elsewhere.

IV. DISCUSSION AND CONCLUSIONS

A big advantage of the (^{3}He)-DT heating scenario is that it gradually converts to $\omega=2\omega_{c\rm T}$ heating, without any change in the ICRF frequency. Thus, ^{3}He is needed only during the ramp-up phase of the pulse and its puff can be switched off once the plasma temperature is high enough for second harmonic tritium heating to become relatively strong. Good performance of this scenario has been proven experimentally and if the availability of ^{3}He is not problematic, this scenario should be considered as the main option for ITER.

The results of our studies show that there is a good backup option, especially for the very early heating stage of the pulse. The design of the ITER ICRF system currently envisages the use of two antennas [24, 25]. With that, one could imagine several ICRF strategies for the ramp-up phase. For example, an interesting option would be to start a pulse with one antenna operating at 37–38 MHz (or 40 MHz) and selectively heat Be impurities. When the plasma pre-heating with the first antenna gets efficient, one can switch on the second antenna at 53 MHz and start ^{3}He puffing to increase T_i further. The first antenna is then switched off and the ICRF system is configured to launch the RF power at a higher frequency later on (e.g., either for $\omega=2\omega_{c\rm T}$ heating or for current drive to extend the pulse length). In any case, by using the first antenna at 37–40 MHz when T_i is low, one can reduce the total consumption of ^{3}He during the ramp-up phase.

For ITER operating at full magnetic field $B_0=5.3$ T, the proposed (Be)-D-T ICRF scenario requires $f\approx 37$ MHz to achieve heating close to the plasma center. At first glance, this frequency is not ITER-relevant since the official ICRF range is $f=40-55$ MHz [24, 25]. However, ITER RF generators are foreseen to deliver RF power in the range $f=35-65$ MHz [39]. Furthermore, according to the computed ICRF antenna performance in ITER, the reduction of the plasma coupling if operating at a lower frequency is reasonably small. If compared to the results for the officially approved frequency 40 MHz, the coupled power is lower by about 15% only for $f=38$ MHz and by 20% for 37 MHz [24, 40, 41].

Yet, if the extension of the frequency range for ITER is not possible, operating at $f=40$ MHz sets no major physics limitations for the proposed (Be)-D-T scenario. A drawback of such operation is the non-central power deposition, with the heating maximum shifted about 60 cm to the high field side ($r/a\approx 0.3-0.35$). Also for this configuration, one can expect a stronger effect of parasitic alpha-particle absorption since at this frequency the IC resonance of D and ^{4}He ions is located centrally. Direct absorption of ICRF power by energetic alpha particles is a potential showstopper for the (Be)-D-T heating scenario at higher T_i. Using the recently upgraded version of the TORIC code [42], we have estimated that this absorption is reasonably small up to $T_0\simeq 10-15$ keV: at $T_0=10/15$ keV the fraction of alpha-particles in the plasma core is computed to be about 0.2%/0.5% and they absorb $p_\alpha\approx 7\%/19\%$ ($p_{\rm Be}=72\%/52\%$) of the incoming RF power, respectively. However, channeling of fusion alpha-particle power using minority ion catalysis [43] could potentially facilitate the application of Be impurity heating in D-T plasmas at higher T_0.

We want to outline a few examples of the three-ion ICRF heating in D-T plasmas already reported in the literature:

(a) During the first D-T experiments in TFTR, reaching localized electron heating and driving non-inductive current via mode conversion, was found to be unsuccessful. The reason for that was attributed to the presence of lithium impurities in the plasma [23]. Numerical computations showed that most of the RF power was absorbed by ^{7}Li ions ($X_{^7\rm Li}\approx 0.5\%$). This

absorption was considered as parasitic, and extensive wall conditioning with ^{6}Li-enriched pellets was used later to eliminate this effect and recover normal MC heating.
(b) For the JET pulse 42769, Start et al. reported $X_{\rm Be} \approx 1.5\%$. It was estimated that the Be impurities were absorbing about 40% of the RF power [11]. Such a non-negligible Be heating was observed even though the IC resonance of Be impurities was located off-axis and although the used D:T ratio ($X_{\rm D} = 18\%$) was quite different to the optimal values we have computed.
(c) In Ref. [3] (Fig. 7), dominant absorption of RF power by Be ions in D:T=1:1 ITER plasmas was computed for $X_{\rm Be} = 1\%$, $f = 40$ MHz and $k_{\|}^{(\rm ant)} = 4$ m^{-1}.
(d) In recent papers, where the ICRF scenarios for the activated phase of ITER were studied, a significant impurity absorption, mostly by argon, was reported [8, 9]. Because the ICRF frequency was chosen to locate the ^{3}He resonance centrally, the argon resonance was placed at the very high field side edge. Note that fully ionized argon ions have a charge-to-mass ratio ($Z/A = 0.45$) very similar to that of Be ions. Again this impurity absorption was considered as a parasitic effect; however, in [9] it was outlined that this effect deserves further investigation with respect to the ICRF operation in ITER.

As follows from the examples shown above and using the reported results, one can conclude that Be can be a very important species for future JET and ITER D-T experiments involving ICRF heating. In view of ITER, this scheme can be tested during the forthcoming DTE2 campaign at JET [44]. For JET operating at $B_0 = 3.6$ T, ICRF heating of Be impurities in D-T plasmas requires the lowest frequency available for the A2 antennas $f = 25$ MHz.

Finally, the proposed $N = 1$ impurity heating scenario in D-T plasmas is relevant for DEMO and future fusion reactors. In fact, there are several choices for the resonant absorber species in D-T plasmas. If for any reason Be can not be used as a wall material for the tokamak-reactor DEMO, this can be equally replaced with the other impurities with a similar charge-to-mass ratio, viz. ^{7}Li^{3+} (ionization energy for the Li$^{2+} \rightarrow$ Li^{3+} transition is $\mathcal{E}_{\rm ion.} = 122$ eV [45]), ^{22}Ne^{10+} ($\mathcal{E}_{\rm ion.} = 1.4$ keV), ^{40}Ar^{17+} ($\mathcal{E}_{\rm ion.} = 4.1$ keV) and ^{40}Ar^{18+} ($\mathcal{E}_{\rm ion.} = 4.4$ keV), etc. Note that the abundance of lithium is no problem for a fusion reactor, and argon and neon are likely to be available for gas puffing as these noble gases can be used for impurity seeding and controlling the deposition of the heat load in a machine.

Summarizing the arguments, the reported results show that heavy intrinsic impurities with $1/3 < Z/A < 1/2$ can be an efficient absorber of the ICRF power in D-T plasmas, and such a resonant impurity RF heating can be used for increasing the bulk ion temperature T_i during the ramp-up phase of the plasma pulse.

Acknowledgements. *The authors are grateful to the anonymous referee for his/her valuable suggestion to clarify the effect of extra impurity species. This work has been carried out within the framework of the EUROfusion Consortium and has received funding from the Euratom research and training programme 2014-2018 under grant agreement No 633053. The views and opinions expressed herein do not necessarily reflect those of the European Commission.*

[1] V. Bergeaud, L.-G. Eriksson and D.F.H. Start, *Nucl. Fusion* **40**, 35–51 (2000).
[2] L.-G. Eriksson, G.T. Hoang and V. Bergeaud, *Nucl. Fusion* **41**, 91–97 (2001).
[3] D. Van Eester, F. Louche and R. Koch, *Nucl. Fusion* **42**, 310–328 (2002).
[4] ITER Physics Expert Group on Energetic Particles, Heating and Current Drive and ITER Physics Basis Editors, *Nucl. Fusion* **39**, 2495–2539 (1999).
[5] M. Porkolab, A. Bécoulet, P.T. Bonoli, C. Gormezano, R. Koch, R.J. Majeski, A. Messiaen, J.M. Noterdaeme, C. Petty, R. Pinsker, D. Start and R. Wilson, *Plasma Phys. Control. Fusion* **40**, A35–A52 (1998).
[6] T.H. Stix, *Plasma Phys.* **14**, 367–384 (1972).
[7] L.-G. Eriksson, M.J. Mantsinen, V.P. Bhatnagar, A. Gondhalekar, C. Gormezano, P.J. Harbour, T. Hellsten, J. Jacquinot, H.J. Jäckel, K. Lawson, C.G. Lowry, E. Righi, G.J. Sadler, B. Schunke, A.C.C. Sips, M.F. Stamp and D.F.H. Start, *Nucl. Fusion* **39**, 337–352 (1999).
[8] R.V. Budny, L. Berry, R. Bilato, P. Bonoli, M. Brambilla, R.J. Dumnot, A. Fukuyama, R. Harvey, E.F. Jaeger, K. Indireshkumar, E. Lerche, D. McCune, C.K. Phillips, V. Vdovin, J. Wright and members of the ITPA-IOS, *Nucl. Fusion* **52**, 023023 (2012).
[9] R.J. Dumont and D. Zarzoso, *Nucl. Fusion* **53**, 013002 (2013).
[10] The JET and TFTR Teams (presented by D.F.H. Start), *Plasma Phys. Control. Fusion* **40**, A87–A103 (1998).
[11] D.F.H. Start, J. Jacquinot, V. Bergeaud, V.P. Bhatnagar, S.W. Conroy, G.A. Cottrell, S. Clement, G. Ericsson, L.-G. Eriksson, A. Fasoli, V. Fuchs, A. Gondhalekar, C. Gormezano, G. Gorini, G. Grosshoegf, K. Guenther, P.J. Harbour, R.F. Heeterg, L.D. Horton, A.C. Howman, H.J. Jäckel, O.N. Jarvis, J. Källne, C.N. Lashmore Davies, K.D. Lawson, C.G. Lowry, M.J. Mantsinen, F.B. Marcus, R.D. Monk, E. Righi, F.G. Rimini, G.J. Sadler, G. Saibene, R. Sartori, B. Schunke, S.E. Sharapov, A.C.C. Sips, M.F. Stamp, M. Tardocchi and P. van Belle, *Nucl. Fusion* **39**, 321–336 (1999).
[12] JET team (prepared by C.A. Cottrell and F.G. Rimini), *Nucl. Fusion* **39**, 2025–2032 (2000).
[13] J.R. Wilson, C.E. Bush, D. Darrow, J.C. Hosea, E.F. Jaeger, R. Majeski, M. Murakami, C.K. Phillips, J.H. Rogers, G. Schilling, J.E. Stevens, E. Synakowski and G. Taylor, *Phys. Rev. Lett.* **75**, 842–845 (1995).
[14] C.K. Phillips, M. Bell, R.E. Bell, S. Bemabei, E. Fredrickson, J.C. Hosea, B.P. LeBlanc, R. Majeski, S. Medley, M. Ono, G. Schilling, E. Synakowski,

G. Taylor, J.R. Wilson and the TFTR Team, *AIP Conf. Proc.* **485**, 69–78 (1999).
[15] D. Shea and D. Morgan, "The Helium-3 Shortage: Supply, Demand, and Options for Congress", Congressional Research Service, CRS Report for Congress (2010);
on-line: http://www.fas.org/sgp/crs/misc/R41419.pdf
[16] M. Porkolab, *AIP Conf. Proc.* **314**, 99–127 (1994).
[17] T.H. Stix, "Waves in Plasmas" (New York: AIP) (1992).
[18] M. Mantsinen, M.-L. Mayoral, D. Van Eester, B. Alper, R. Barnsley, P. Beaumont, J. Bucalossi, I. Coffey, S. Conroy, M. de Baar, P. de Vries, K. Erents, A. Figueiredo, A. Gondhalekar, C. Gowers, T. Hellsten, E. Joffrin, V. Kiptily, P.U. Lamalle, K. Lawson, A. Lyssoivan, J. Mailloux, P. Mantica, F. Meo, F. Milani, I. Monakhov, A. Murari, F. Nguyen, J.-M. Noterdaeme, J. Ongena, Yu. Petrov, E. Rachlew, V. Riccardo, E. Righi, F. Rimini, M. Stamp, A.A. Tuccillo, K.-D. Zastrow, M. Zerbini and JET EFDA contributors, *Nucl. Fusion* **44**, 33–46 (2004).
[19] T.H. Stix, *Nucl. Fusion* **45**, 737–754 (1975).
[20] Ye.O. Kazakov, D. Van Eester, R. Dumont and J. Ongena, *Nucl. Fusion* **55**, 032001 (2015).
[21] S. Brezinsek and JET-EFDA Contributors, *J. Nucl. Mat.* **463**, 11–21 (2015).
[22] S. Brezinsek, A. Widdowson, M. Mayer, V. Philipps, P. Baron-Wiechec, J.W. Coenen, K. Heinola, A. Huber, J. Likonen, P. Petersson, M. Rubel, M.F. Stamp, D. Borodin, J.P. Coad, A.G. Carrasco, A. Kirschner, S. Krat, K. Krieger, B. Lipschultz, Ch. Linsmeier, G.F. Matthews, K. Schmid and JET contributors, *Nucl. Fusion* **55**, 063021 (2015).
[23] J.R. Wilson, R.E. Bell, S. Bernabei, K. Hill, J.C. Hosea, B. LeBlanc, R. Majeski, R. Nazikian, M. Ono, C.K. Phillips, G. Schilling and S. von Goeler, *Phys. Plasmas* **5**, 1721–1726 (1998).
[24] P.U. Lamalle, B. Beaumont, T. Gassman, F. Kazarian, B. Arambhadiya, D. Bora, J. Jacquinot, R. Mitteau, F.C. Schiiller, A. Tanga, U. Baruah, A. Bhardwaj, R. Kumar, A. Mukherjee, N.P. Singh, R. Singh, R. Goulding, D. Rasmussen, D. Swain, G. Agarici, R. Sartori, A. Borthwick, A. Davis, J. Fanthome, C. Hamlyn-Harris, A.D. Hancock, A. Kaye, D. Lockley, M. Nightingale, P. Dumortier, F. Durodie, D. Grine, R. Koch, F. Louche, A. Lyssoivan, A. Messiaen, P. Tamain, M. Vervier, R.R. Weynants, R. Maggiora, D. Milanesio, F. Braun, J-M. Noterdaeme, K. Vulliez, *AIP Conf. Proc.* **1187**, 265–268 (2009).
[25] J.R. Wilson and P.T. Bonoli, *Phys. Plasmas* **22**, 021801 (2015).
[26] Ye.O. Kazakov, T. Fülöp and D. Van Eester, *Nucl. Fusion* **53**, 053014 (2013).
[27] D. Van Eester and R. Koch, *Plasma Phys. Control. Fusion* **40**, 1949–1975 (1998).
[28] R.J. Dumont *AIP Conf. Proc.* **1187**, 97–100 (2009).
[29] M. Brambilla, *Plasma Phys. Control. Fusion* **41**, 1–34 (1999).
[30] R. Bilato, M. Brambilla, O. Maj, L.D. Horton, C.F. Maggi and J. Stober, *Nucl. Fusion* **51**, 103034 (2011).
[31] R.J. Dumont, *Nucl. Fusion* **49**, 075033 (2009).
[32] M.-L. Mayoral, P.U. Lamalle, D. Van Eester E.A. Lerche, P. Beaumont, E. De La Luna, P. De Vries, C. Gowers, R. Felton, J. Harling, V. Kiptily, K. Lawson, M. Laxåback, P. Lomas, M.J. Mantsinen, F. Meo, J.-M. Noterdaeme, I. Nunes, G. Piazza, M. Santala and JET EFDA contributors, *Nucl. Fusion* **46**, S550–S563 (2006).
[33] P.U. Lamalle, M.J. Mantsinen, J.-M. Noterdaeme, B. Alper, P. Beaumont, L. Bertalot, T. Blackman, Vl.V. Bobkov, G. Bonheure, J. Brzozowski, C. Castaldo, S. Conroy, M. de Baar, E. de la Luna, P. de Vries, F. Durodie, G. Ericsson, L.-G. Eriksson, C. Gowers, R. Felton, J. Heikkinen, T. Hellsten, V. Kiptily, K. Lawson, M. Laxåback, E. Lerche, P. Lomas, A. Lyssoivan, M.-L. Mayoral, F. Meo, M. Mironov, I. Monakhov, I. Nunes, G. Piazza, S. Popovichev, A. Salmi, M.I.K. Santala, S. Sharapov, T. Tala, M. Tardocchi, D. Van Eester, B. Weyssow and JET EFDA contributors, *Nucl. Fusion* **46**, 391–400 (2006).
[34] Ye.O. Kazakov, I.V. Pavlenko, D. Van Eester, B. Weyssow and I.O. Girka, *Plasma Phys. Control. Fusion* **52**, 115006 (2010).
[35] D. Van Eester, E. Lerche, T.J. Johnson, T. Hellsten, J. Ongena, M-L. Mayoral, D. Frigione, C. Sozzi, G. Calabro, M. Lennholm, P. Beaumont, T. Blackman, D. Brennan, A. Brett, M. Cecconello, I. Coffey, A. Coyne, K. Crombe, A. Czarnecka, R. Felton, M. Gatu Johnson, C. Giroud, G. Gorini, C. Hellesen, P. Jacquet, Ye. Kazakov, V. Kiptily, S. Knipe, A. Krasilnikov, Y. Lin, M. Maslov, I. Monakhov, C. Noble, M. Nocente, L. Pangioni, I. Proverbio, M. Stamp, W. Studholme, M. Tardocchi, T.W. Versloot, V. Vdovin. A. Whitehurst, E. Wooldridge, V. Zoita and JET EFDA Contributors, *Plasma Phys. Control. Fusion* **54**, 074009 (2012).
[36] Ye.O. Kazakov, V.G. Kiptily, S.E. Sharapov, D. Van Eester and JET-EFDA Contributors, *Nucl. Fusion* **52**, 094012 (2012).
[37] T. Pütterich, R. Dux, R. Neu, M. Bernert, M.N.A. Beurskens, V. Bobkov, S. Brezinsek, C. Challis, J.W. Coenen, I. Coffey, A. Czarnecka, C. Giroud, P. Jacquet, E. Joffrin, A. Kallenbach, M. Lehnen, E. Lerche, E. de la Luna, S. Marsen, G. Matthews, M.-L. Mayoral, R.M. McDermott, A. Meigs, J. Mlynar, M. Sertoli, G. van Rooij, the ASDEX Upgrade Team and JET EFDA Contributors, *Plasma Phys. Control. Fusion* **55**, 124036 (2013).
[38] M. Brambilla, *Nucl. Fusion* **34**, 1121–1143 (1994).
[39] F. Kazarian, B. Beaumont, A. Arambhadiya, T. Gassmann, Ph. Lamalle, D. Rathi, A. Mukherjee, P. Ajesh, H. Machchhar, D. Patadia, M. Patel, K. Rajnish, R. Singh, G. Suthar, R. Trivedi, R. Kumazawa, T. Seki, K. Saito, H. Kasahara, T. Mutoh, F. Shimpo and G. Nomura, *Fusion Eng. Design* **86**, 888–891 (2011).
[40] A. Messiaen, R. Koch, R.R. Weynants, P. Dumortier, F. Louche, R. Maggiora and D. Milanesio, *Nucl. Fusion* **50**, 025026 (2010).
[41] B. Beaumont, T. Gassmann, F. Kazarian, P. Lamalle, D. Rasmussen, A. Mukherjee, U. Baruah, R. Sartori, "ITER ICRF system: R&D progress and technical choices", *Proc. 23rd IEEE/NPSS Symp. on Fusion Engineering SOFE 2009* (San Diego, CA, 2009);
http://dx.doi.org//10.1109/FUSION.2009.5226425
[42] M. Brambilla and R. Bilato, *Nucl. Fusion* **55**, 023016 (2015).
[43] A.I. Zhmoginov and N.J. Fisch, *Phys. Rev. Lett.* **107**, 175001 (2011).

[44] Ye.O. Kazakov, D. Van Eester, E. Lerche, J. Ongena and R. Dumont, "Enhanced D-T bulk ion heating via minority beryllium ICRF scenario", *JET Task Force Meeting, 06 January 2015*; online http://users.euro-fusion.org/pages/tfiospti/TFmeetings/2015/20150106/Kazakov_060115.pdf

[45] http://en.wikipedia.org/wiki/Ionization_energies_of_the_elements_(data_page)